2024 IEEE International Conference on Robotics and Automation (ICRA 2024)
May 13-17, 2024. Yokohama, Japan

Design and Evaluation of a Reconfigurable 7-DOF Upper Limb Rehabilitation Exoskeleton with Gravity Compensation

Linliang Zheng, Qingcong Wu, *Member*, *IEEE*, Yanghui Zhu, *Student Member*, *IEEE*, and Qiang Zhang

Abstract— **With the development of society, aging population and the number of stroke patients is increasing year by year. Rehabilitation exoskeleton can help patients to carry out rehabilitation training and improve their activities of daily living (ADL). First of all, a reconfigurable exoskeleton for upper limb rehabilitation is designed in this paper. The exoskeleton combines gravity compensation with left-right arm switching function through its reconfigurability. Secondly, the motion space and singular configuration of the exoskeleton are analyzed. By changing the working mode of the gravity compensation device, the control experiment of the motor is carried out. The influence of gravity compensation device on motor driving torque and energy consumption is analyzed. Finally, the results of experiment show that, in the best case, the gravity compensation device can reduce the energy consumption by 41.15% and the maximum motor current by 33.56% of the driving element.**

I. Introduction

According to the survey, there are about 13.7 million new stroke patients worldwide each year, most of whom are middle-aged and elderly [1,2]. Traditional rehabilitation therapy requires the professional skills of rehabilitation trainers for training, and the patient is in a passive state. However, this process consumes a lot of physical energy for trainers, and rehabilitation training is also subject to the working time and human resources of rehabilitation trainers [3]. Exoskeleton robots generally refer to mechanical devices that are similar to the corresponding parts of the human body. But they still need human leadership in control and cannot achieve autonomous control [4,5,6]. With the progress of The Times and the maturity of robot development and control technology, upper limb rehabilitation robots have been able to gradually replace rehabilitation trainers [7,8,9]. These robots can provide more targeted treatment for patients with impaired upper limb function [10,11].

More and more exoskeletons for upper limb rehabilitation have been developed, the AGREE exoskeleton designed by Dalla Gasperina et al. can be used with both the left and right arms [12]. The rehabilitation exoskeleton uses a spring-pulley anti-gravity system to minimize torque requirements. However, the spring-pulley anti-gravity system on this exoskeleton can only provide a maximum torque demand of 25%. The performance requirements for the motors are still extremely high. Fallaha et al. developed an upper limb rehabilitation exoskeleton robot [13], which can realize left-arm and right-arm interchange. However, there is no gravity balancing device designed in the structure, increasing the performance requirements for the motor. Kim et al. developed a passive upper limb exoskeleton using a spring to passively generate assistive torque [14]. The exoskeleton can generate 9.5 NM of maximum assistive torque at 120° to assist overhead task with a 1-kg tool. However, the assistive mechanism accounts for a large part of the overall structure, and the exoskeleton is only limited to one side. And Yves Zimmermann and others designed an upper limb rehabilitation exoskeleton called ANYexo 2.0[15]. Li et al. designed a 5-DOF upper limb exoskeleton for rehabilitation [16]. Cheng et al designed a portable upper-limb elbow-forearm exoskeleton [17]. None of the three upper limb rehabilitation exoskeletons mentioned the concept of gravity balance and left-right switching. It can be found that the existing upper limb rehabilitation exoskeleton robots and passive upper limb exoskeletons rarely combine gravity balance with mechanism reconfiguration or left-right arm switching function in structure. And in the exoskeleton robots with both functions, the compensation device provides less torque.

Based on the above discussion, in this paper, we combine gravity compensation, reconfiguration, and left-arm and right-arm switching, aiming to develop a new reconfigurable upper limb rehabilitation exoskeleton. The main contributions of this article are as follows:

1) A reconfigurable upper limb rehabilitation exoskeleton combined with gravity compensation is proposed. The exoskeleton can use its reconfigurability to switch between the left and right arms of the exoskeleton and the gravity compensation device. The gravity compensation device can reduce the requirement of motor control performance and energy consumption.
2) The Monte Carlo method, the D-H parameter method and the method of unit vector mixed product are used to prove that the exoskeleton has a large working space and there is no singular configuration.
3) The gravity compensation device installed on the exoskeleton was evaluated through experiments, and its impact on joint motor trajectory tracking and energy consumption was analyzed.

*Research supported in part by the National Natural Science Foundation of China under Grant 52175014, in part by the Key Research and Development Program of Jiangsu Province (Social Development) under Grant BE2023813, in part by the Natural Science Foundation of Jiangsu Province under Grant BK20211183, and in part by the Postgraduate Research & Practice Innovation Program of NUAA under Grant xcxjh20230513.

Linliang Zheng, Qingcong Wu, Yanghui Zhu and Qiang Zhang are with the College of Mechanical and Electrical Engineering, Nanjing University of Aeronautics and Astronautics, Nanjing 210016, Jiangsu, China (corresponding author: wuqc@nuaa.edu.cn).

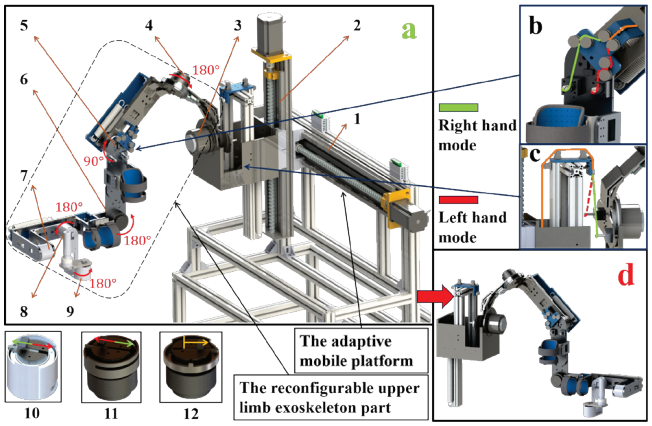

Figure 1. Reconfigurable 7-DOF upper limb rehabilitation exoskeleton with gravity compensation: (a) exoskeleton left-arm mode. (b) switch the spring connection point of the gravity compensation device at shoulder joint (abduction/adduction). (c) switch the spring connection point of the gravity compensation device at shoulder joint (flexion/extension). (d) exoskeleton right-arm mode. 1. x-axis degree of freedom; 2. y-axis degree of freedom; 3. abduction/adduction of shoulder joint; 4. external/internal rotation of shoulder joint; 5. flexion/extension of shoulder joint; 6. flexion/extension of elbow joint; 7. pronation/supination of elbow joint; 8. ulnar/radial flexion of wrist joint; 9. flexion/extension of wrist joint; 10. single-layer bidirectional limit device (apply to 7/8/9); 11. double-layer bidirectional limit device (apply to 3/5); 12. single-layer unidirectional limiting device (apply to 4/6).

The remainder of this paper is organized as follows. In section II, the exoskeleton structure and reconfigurability are introduced. The experiment and experimental results are introduced in section III. At the end, Section IV concludes this paper.

II. System Description

The model of the upper limb rehabilitation exoskeleton is shown in Fig. 1. The exoskeleton uses 7 degrees of freedom to fit the movement of the human upper limb, corresponding to shoulder abduction/adduction, external/internal rotation, and flexion/extension, elbow flexion/extension and pronation/supination, wrist ulnar/radial flexion and flexion/extension [see Fig. 1 (3)-(9)]. The exoskeleton can realize the function of left-arm and right-arm switching by reconfiguration. The gravity compensation device on the exoskeleton can also be reconstructed to adapt to the left or right arms. By deflecting the axes of the shoulder joint with rotational degrees of freedom, the occurrence of singular configurations in the exoskeleton can be avoided.

A. Exoskeleton with Reconfigurability and Adaptability

The main structure of the exoskeleton consists of two parts, namely, the reconfigurable upper limb exoskeleton and the adaptive mobile platform, as shown in Fig.1 (a). The reconfigurable upper limb exoskeleton is used to achieve the main rehabilitation training functions. The adaptive mobile platform is an adjustment mechanism that can assist in left-right mode switching and is used to adapt to the patient's body type. The exoskeleton is equipped with a six-dimensional force-torque sensor at the wrist joint, which is used to perceive the user's intention and carry out corresponding motion intention recognition.

The reconfigurable upper limb exoskeleton can switch the structure from right-arm mode [see Fig. 1 (a)] to left-arm mode [see Fig. 1 (d)] by changing the rotating joint and rotation angle. The rotation angles (marked in red) of each joint motor are shown in Fig. 1 (a). The left-arm and right-arm modes are completely mirrored after switching. Each driving element of the exoskeleton is equipped with a limiting device. There are diverse types of limiting devices at different joints, as shown in Fig. 1 (10)-(12). These limiting devices can be adapted to switch between left-arm and right-arm modes of the exoskeleton. The reconfigurable exoskeleton is fitted with a gravity compensation device. When the exoskeleton switches between left and right arms, the connection point of the gravity compensation device needs to be adjusted, as shown in Fig. 1 (b)(c). The exoskeleton is reconstructed to complete the left-right arm switching function without affecting the use of the gravity compensation device.

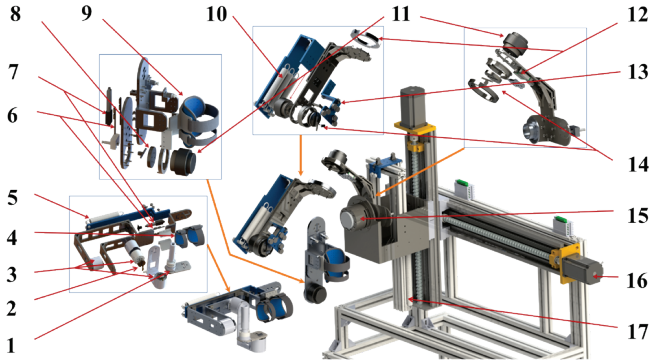

Figure 2. Explosion diagram of the internal structure of the upper limb exoskeleton: 1. six-dimensional force-torque sensor; 2. forearm limit device; 3. joint motor; 4.forearm wearable parts; 5. forearm spring; 6. linear slider and guide rail; 7. linear actuator; 8. upper arm limit device; 9. upper arm wearable parts; 10. upper arm spring; 11. joint motor; 12. brake device; 13. guide device; 14. shoulder joint limit device; 15. joint motor; 16. servo motor; 17. shoulder joint spring.

As shown in Fig. 2, the internal assembly of the upper limb rehabilitation exoskeleton can be seen. The mechanism follows the lightweight design criteria and needs to satisfy certain stiffness requirements. The center of gravity of the connecting rods and drive is as close to the rotating axis as possible to reduce the inertia during rotation. The forearm and upper arm of the exoskeleton have straps that can be connected with the forearm and upper arm of the user. The position and tension of the straps can be adjusted to improve comfort [see Fig. 2 (4)(9)]. Mechanical limiting devices are used in all driving elements to prevent the movement of the mechanism beyond the maximum limit range.

In addition to the above human-machine connection components. The length of the connecting rods in the forearm and upper arm of the exoskeleton can be changed and locked by linear actuators. The connecting rod in the palm part can achieve stepless adjustment between the palm and the wrist by mechanical locking. The previously mentioned adaptive mobility platform realizes horizontal and vertical movement through two vertically connected ball screw slideways. It can adjust the initial position of the entire exoskeleton to adapt to different types of seats and people of different heights. Through the institutions mentioned above, the exoskeleton can adapt to the needs of most people of 1.6m~1.8m in height.

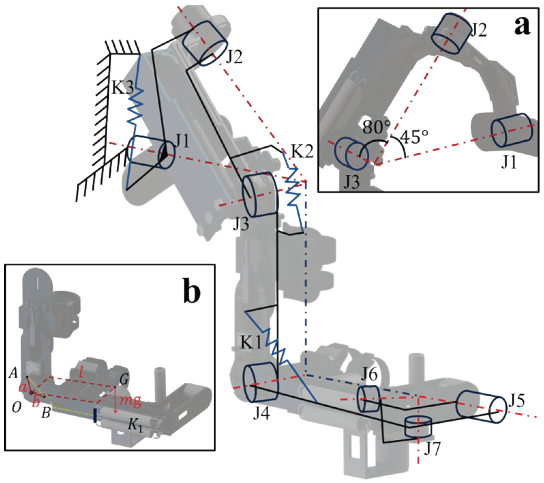

Figure 3. Reconfigurable upper limb rehabilitation exoskeleton and part of the gravity compensation principle model: (a) the rotation axis angle set at the shoulder joint of the exoskeleton (b) gravity compensation principle model at J4.

B. Gravity Compensation System

The influence of gravity on the robot is mainly manifested as the bias torque, which causes the robot's various moving joints to be constantly affected. And the influence of the gravity will change with the change of different postures and positions of the mechanical structure. In some limit positions, the bias torque sometimes exceeds the maximum output torque of the robot drive device, which may cause the robot to lose control and cause serious safety accidents. Therefore, it is very necessary to design an effective balancing mechanism to compensate the biased torque to improve the working and safety performance of the robot [18-19]. Considering the reconfigurability of the exoskeleton, the gravity compensation device is symmetrically designed for the upper limb rehabilitation exoskeleton described in this paper. The following paper introduces the design principle of gravity compensation device.

Fig. 3 is a structural diagram of the zero-free-length spring [20] gravity compensation device designed for the three joints (J1, J3 and J4)). The joints J1-J7 mentioned in the figure correspond to (3)-(9) in Fig. 1 respectively. The gravity compensation devices are structurally compatible with the left-right arm switching function. The balance principle of the three joints is the same. Taking joint J4 as an example, the whirling arm [see Fig. 3 (b)] includes the front joints (J5, J6 and J7) and all the connections between them.

As shown in Fig. 3 (b), it can be assumed that all the generated gravity at the whirling arm is mg. The moment arm of force is l, and torque M_1 will be generated at the rotation center O of joint J4. The relationship is expressed as (1).

$$M_1 = mgl\sin\theta \tag{1}$$

For the spring, it can be assumed that it generates torque M_2 at the rotation center O of joint J4. M_2 can be expressed by the total stiffness K_1 of the spring, the original length x_0, the actual length x, the distance a between the center of rotation O and the connection point A of the relative fixed connecting rod, the distance b from the center of rotation O to the initial stretch position B of the spring, and the relative angle θ

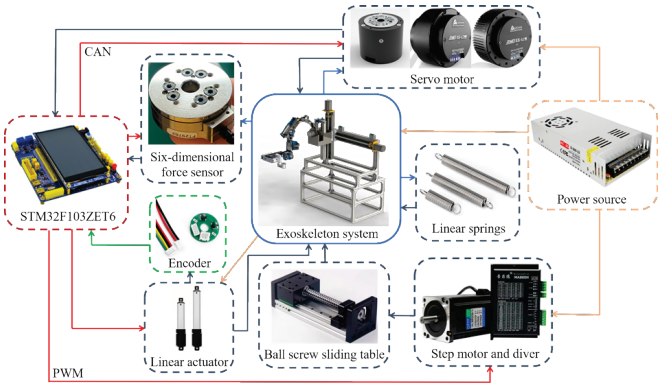

Figure 4. Exoskeleton control system.

between the front link and the back end relative to the fixed link. The relationship is expressed as (2).

$$M_2 = \frac{abK_1(x-x_0)\sin\theta}{x} \tag{2}$$

M_2 is the gravity compensation torque generated by the zero-free-length spring. Since the initial elongation position of the spring in the model coincides with point B of the fixed pulley, the gravity compensation torque can be expressed as M_2' (3), and the conclusion (4) can be finally obtained.

$$M_2' = abK_1\sin\theta \tag{3}$$

$$M_1 = M_2', K_1 = \frac{mgl}{ab} \tag{4}$$

At this time, the spring stiffness K_1 is a fixed value and does not change with the movement of the mechanical arm, that is, the state of gravity balance is reached. Using similar modeling and calculation as above, the other two spring stiffness (K_2, K_3) can be obtained.

In the initial position of the mechanism, the device can achieve gravity balance. In the process of multi-joint composite motion of the mechanism, the device can achieve gravity compensation. It can reduce the performance requirements of the drive motor and improve the usage performance of the motor. In the following paper, the actual effect of the device will be verified by control experiments.

C. Exoskeleton Control System

The control system of the upper limb rehabilitation exoskeleton is shown in Fig. 4. The core control component of the system is a single-chip microcomputer STM32F103ZET6. The control component uses CAN communication to control the operation of the joint motors to affect the configuration of the entire structure. The control element can control the step motors BYG250 (PERFECT, China) and divers MA860H (PERFECT, China) to change the position of the ball screw slide table. The type of the servo motors at the wrist joint is DM-J4310-2EC (dmBot, China). The servo motors RMD-X6-S2 (MYACTUATOR, China) are installed at two shoulder joints and one elbow joint. The control element can recognize the intention and detect the human-machine interaction force through the six-dimensional force-torque sensor Mini45 (ATI Industrial Automation, USA), so as to control the operation of the exoskeleton and ensure the safety of human-machine interaction. In the last position of the shoulder joint, the type of the servo motor is RD-X8-S2 (Myactuator, China). The linear actuators (Luilec, China) are also directly controlled by

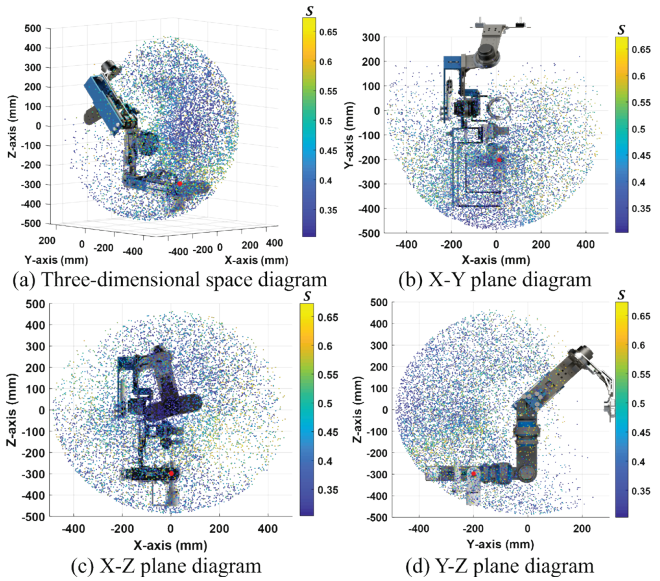

(a) Three-dimensional space diagram (b) X-Y plane diagram

(c) X-Z plane diagram (d) Y-Z plane diagram

Figure 5. Upper limb exoskeleton workspace and singularity.

the control element, the control element uses its built-in encoder to read the actual position of the linear actuator, and more accurately adjust the length of the upper arm and forearm of the exoskeleton.

D. Working Space and Singular Configuration

The designed exoskeleton actuator can be simplified into a series robot composed of 7 rotating pairs of links. The improved D-H (Denavit-Hartenberg) parameter method [21] is used to establish the spatial coordinate system of each joint. The mapping of joint space to the end actuator is described in Cartesian space.

After measuring the prototype, the parameters of L_1, L_2 and L_3 can be obtained as follows: 261mm, 72mm, 226.5mm. Monte Carlo method [22] and random sampled were used to according to the motion range of each joint, set the number of random sampling points to 10000. Then Monte Carlo cloud point map was calculated and drawn in Cartesian base coordinate system. Fig. 5 shows the three-dimensional diagram and plane diagram of the working space.

To avoid creating singular configurations, this institution adopts the following solutions: Firstly, the first ball-type joint, in the three degrees of freedom of the shoulder joint, is designed as a non-90 degree deflection angle between the two axes [see Fig. 3 (a)]; At the same time, in the second type of spherical hinge joint (composed of two parts of the elbow joint pronation/supination and the wrist joint), the three axes are designed to be vertical in pairs, but because of the small scope of the working space, there is no singular configuration.

Based on the above analysis, it can be concluded that it is difficult for the wrist joint to appear strange configuration, so further singularity analysis of the shoulder joint can directly reflect the singularity of the whole mechanism. Therefore, the singularity of exoskeleton can be analyzed by calculating the intersection of joint axes at point O using the method of unit vector mixed product [23]. The quantization expression of singularity is defined as:

$$S = 1 - |\boldsymbol{z_1} \cdot (\boldsymbol{z_2} \times \boldsymbol{z_3})| \tag{5}$$

In the formula, S is the degree of singularity, z_1, z_2 and z_3 respectively represents the direction vector of the rotation axis of the three degrees of freedom in the shoulder joint.

According to the formula, when $S = 1$, the rotation axis of the three degrees of freedom of the joint is in a coplanar position, that is, a singular configuration. When $S = 0$, the two rotation axes of the three degrees of freedom are perpendicular to each other, that is, the operability is maximum at this time.

The cloud point diagram of shoulder singular configuration can be obtained by equation (5) combined with the workspace distribution solved above, as shown in Fig. 5. In the Fig. 5, each end pose is represented by a different color to indicate the magnitude of its singularity. It can be seen that the maximum value is between 0.65 and 0.7, indicating that there is no singularity pattern at the shoulder joint of this structure.

III. EXPERIMENT

A. Experimental Setup and Data Handling

In order to verify the influence of the gravity compensation device (GCD) on the trajectory tracking and energy consumption of the drive elements on the exoskeleton, we conduct experiments on the upper limb rehabilitation exoskeleton. The experimental process is shown in Fig. 6. The motor trajectory tracking is controlled by PID. By debugging the operation of the motor on the exoskeleton with no load, we find out the suitable PID value (P=90, I=0.1, D=0). We set the sine motion trajectory of the motor in the control element, and let the motor track the trajectory after a subject putting on the exoskeleton. During the operation of the motor, we analyze the performance of the gravity compensation device by recording the position and current of the motor. The subject is 170cm tall and 61kg in weight. This paper focuses on verifying the energy-saving characteristics of gravity balance, and more experiments with subjects will be done in the future work.

For the data of the motor position, we calculate root-mean-square error (RMSE) and the absolute maximum error (AME) between the motor trajectory and the expected trajectory. The calculation methods of RMSE and AME are shown in formula (6) and (7):

$$AME = \max(|X_i|), (i = 1,2,3 \cdots N) \tag{6}$$

$$\overline{X} = \frac{\sum_{i=1}^{N} X_i}{N},\ RMSE = \sqrt{\frac{\sum_{i=1}^{N}(X_i - \overline{X})^2}{N}} \tag{7}$$

In the formulas, $\overline{X}$ is the average value of the difference between the actual motor trajectory and the expected trajectory, X_i is the recorded real-time difference between the actual motor trajectory and the expected trajectory, N is the number of position data collected.

For the data of the motor current, we can calculate the power consumption and analyze the influence of the gravity compensation device in the whole process of the motor. And we calculate the absolute maximum current (AMC) by using the formula (8). The work done by the motors in the whole process could be estimated by using the formula (9):

$$AMC = \max(|I_i|), (i = 1,2,3 \cdots n) \tag{8}$$

$$W = \sum_{i=1}^{n} \frac{U|I_i|t}{n} \tag{9}$$

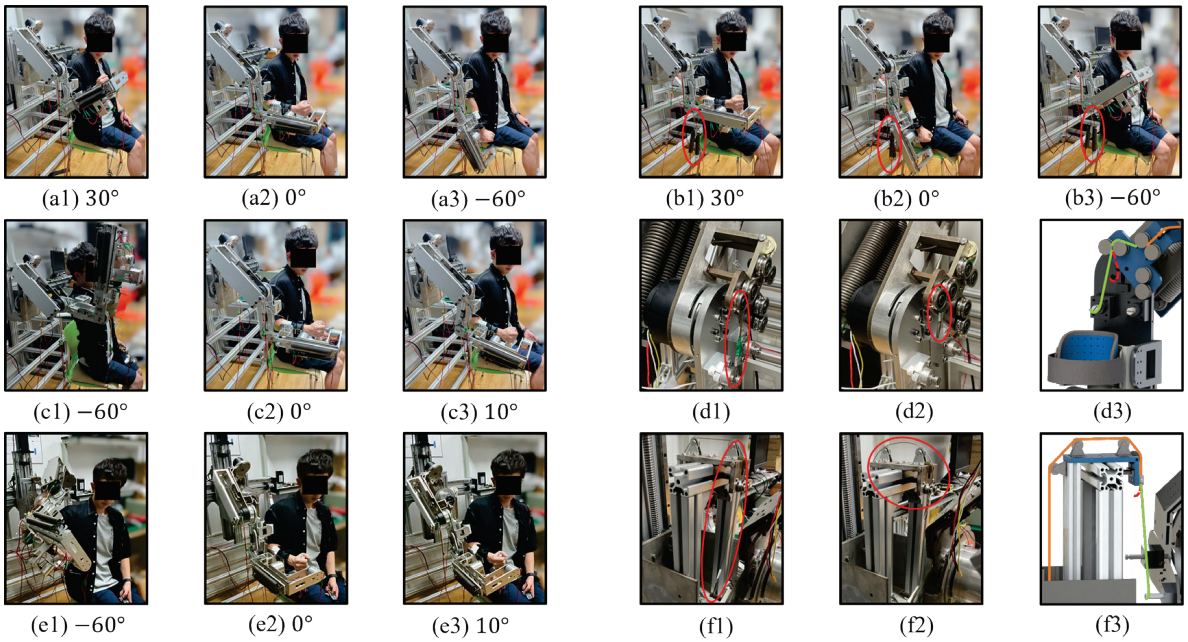

Figure 6. Experiments to detect the influence of gravity compensation device (GCD) on passive rehabilitation training of the exoskeleton: (a1)-(a3) experimental process diagram of passive rehabilitation experiment with GCD (J4); (b1)-(b3) experimental process diagram of passive rehabilitation without GCD (J4); (c1)-(c3) experimental process diagram of passive rehabilitation (J5); (d1) working mode of GCD at joint 5; (d2) non-working mode of GCD at joint 5; (d3) working (green) and non-working (red) model of GCD at joint 5 ;(e1)-(e3) experimental process of passive rehabilitation (J7); (f1) working mode of GCD at joint 7; (f2) non-working mode of GCD at joint 7; (f3) working (green) and non-working (red) model of GCD at joint 7.

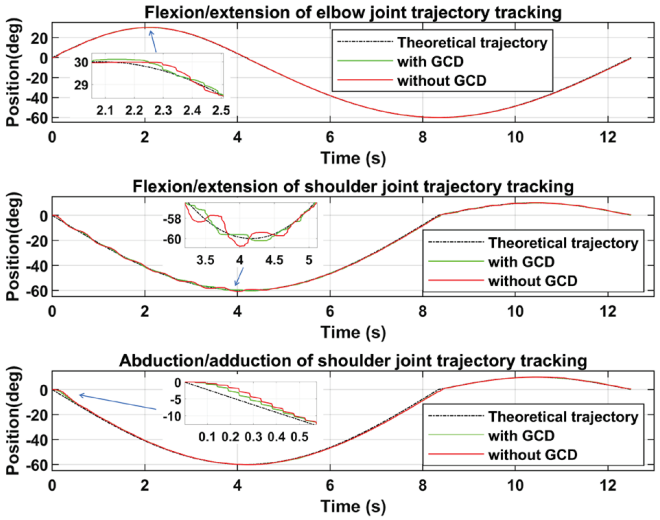

Figure 7. The influence of gravity compensation equipment on trajectory tracking of motor: GCD means gravity compensation device.

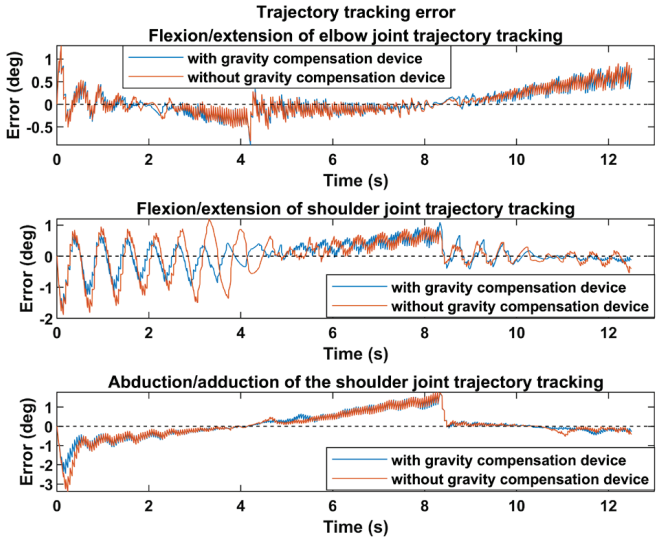

Figure 8. The influence of gravity compensation device on error angle of motor trajectory tracking.

In the formulas, W is the work done by the motor, the voltage U is a constant value 24V. I_i is the recorded real-time motor current of motor, t is the total time of the motor runs, n is the number of motor current data collected.

We conduct two sets of experiments respectively. In experiment 1, the GCD is in working mode, has the effect of gravity compensation, as shown in Fig. 6 (a1)- (a3) (d1) and (f1). The spring in the GCD is connected to the exoskeleton, and the energy can be converted during the trajectory tracking of the drive element. In experiment 2, the GCD is in non-working mode, as shown in Fig. 6 (b1) -(b3), (d2) and (f2). The springs in GCD are in a suspended state, and there is no interaction with the exoskeleton, which does not affect the motor operation. Fig. 6 (d3) and (f3) show the GCD spring connection model of the shoulder joint J1 and J3 [see Fig. 3]. The green line indicates that the spring is connected, the GCD is in working mode; The red line indicates that the spring is in a suspended state, the GCD is in non-working mode.

B. *Experimental result*

We did multiple sets of repeated experiments for each joint, and the experimental results were very similar. We took one set of data for graph analysis. Fig. 7 shows the position tracking performance of the motor with GCD and the motor without GCD at three joints. The experimental results of the tracking errors are shown in Fig. 8, and the experimental data of the motor current are shown in Fig. 9. The specific influence of the GCD on the

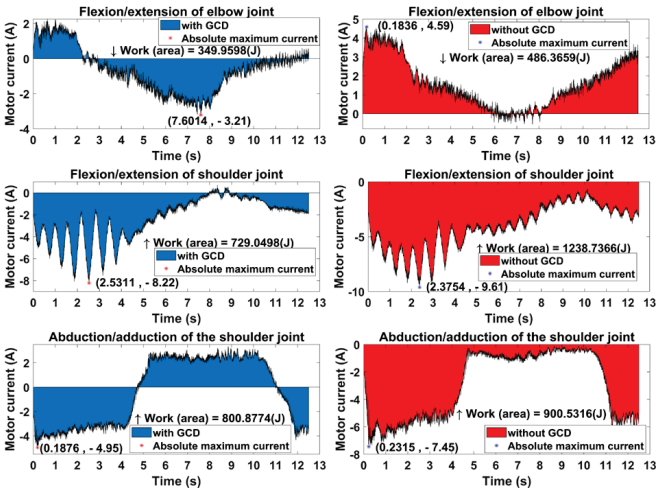

Figure 9. The influence of gravity compensation device on motor energy consumptions. GCD means gravity compensation device.

TABLE I. EXPERIMENTAL DATA ANALYSIS

Joint (GCD mode)		RMSE (deg)	AME (deg)	Work (J)	AMC (A)
FEE	working	0.2741	1.2647	349.9598	3.21
	non-working	0.2801	1.2947	486.3659	4.59
FES	working	0.4120	1.7982	729.0498	8.22
	non-working	0.5459	1.8882	1238.7366	9.61
AAS	working	0.6327	2.4594	800.8774	4.95
	non-working	0.7043	3.3893	900.5316	7.45

three joint motors is analyzed in the Table I. The effect of GCD on motor trajectory tracking can be analyzed by calculating the numerical difference before and after GCD installation, and then dividing by the numerical value before installation.

According to Fig. 8 and Table 1, the experimental results show that the motor trajectory tracking effect is better in GCD in working mode than in non-working mode. At flexion/extension of elbow joint (FEE), RMSE (0.2741° and 0.2801°) and AME (1.2647° and 1.2947°) are reduced by 2.14% and 2.32%, respectively. At flexion/extension of shoulder joint (FES), RMSE (0.4120° and 0.5459°) and AME (1.7983° and 1.8882°) are reduced by 24.53% and 4.76%, respectively. At abduction/adduction of shoulder joint (AAS), RMSE (0.6327° and 0.7043°) and AME (2.4594° and 3.3893°) are reduced by 10.17% and 27.44%, respectively. For RMSE, the decrease is most obvious at FES. For AME, the decrease is most obvious at AAS. Of the three joints, AAS shows the best overall improvement.

According to Fig. 9 and Table 1, the experimental results show that the motor operating condition is better in GCD in working mode than in non-working mode. At FEE, the work (349.9598J and 486.3659J) and AMC (3.21A and 4.59A) are reduced by 28.05% and 30.07%, respectively. At FES, the work (729.0498J and 1238.7366J) and AMC (8.22A and 9.61A) are reduced by 41.15% and 14.46%, respectively. At AAS, the work (800.9774J and 900.5316J) and AMC (4.95A and 7.45A) are reduced by 11.07% and 33.56%, respectively. For the work, the decrease effect is most obvious at FES. The improvement of energy consumption at FES is the greatest, and the decrease of AMC at AAS is the greatest. Of the three joints, FEE shows the best overall improvement.

It can be seen from the result analysis that the gravity compensation devices have a gain effect on motor trajectory tracking, especially at AAS and FES. GCD reduce the root-mean-square error and maximum error respectively, and significantly improve the control accuracy of the motor. Furthermore, GCD in these three places simultaneously reduce the maximum driving torque and energy consumption of the driving components. GCD can effectively reduce the external load borne by the motor and make the motor run more smoothly.

Compared with the AGREE exoskeleton [12], the exoskeleton proposed in this paper has better performance in gravity balance, about 5% and 8% higher in FEE and AAS respectively. And it has more flexible structure and better reconfigurable performance. Compared with the passive upper limb exoskeleton [14,24], the exoskeleton proposed in this paper is relatively low in terms of gravity balance performance, but the exoskeleton has more freedoms and a wider range of applications. Compare with other exoskeletons driven directly by motors without gravity balance or Compensation [13,15,16,17], the exoskeleton mentioned in this paper has relatively lower performance requirements for the motor and lower energy consumption.

IV. CONCLUSION

In this paper, we propose a reconfigurable upper limb rehabilitation exoskeleton combined with gravity compensation. The gravity compensation devices are designed based on the reconfigurability of the exoskeleton and can be combined with the function of switching between left and right arms. Through the modeling of exoskeleton kinematics, the working space and singular configuration of this upper limb exoskeleton are analyzed, and its superior kinematics characteristics are verified. Finally, the proposed upper limb rehabilitation exoskeleton combined with gravity compensation is experimentally verified. The subjects use protective gear and straps on the exoskeleton to fix their unilateral arm to the exoskeleton and adjust the size of the exoskeleton components to solve joint correspondence problems. Rehabilitation training is conducted after gripping the front grip tightly. During clinical rehabilitation training, it is necessary for physicians to guide the use of exoskeletons and use them to provide rehabilitation training for patients. The experimental results show that the gravity compensation devices can optimize the control performance of the motor, greatly reduce the performance requirements of the motor. And they reduce the driving torque and power consumption of the motors. In the follow-up work, we will study the application of impedance admittance and compliance control to the upper limb rehabilitation exoskeleton system and improve the safety performance of the exoskeleton operation.

REFERENCES

[1] M. P. Lindsay et al., "World stroke organization (WSO): Global stroke fact sheet 2019," vol. 14, no. 8, pp. 806–817, 2019.

[2] V. L. Feigin et al., "Global, regional, and national burden of neurological disorders, 1990–2016: A systematic analysis for the global burden of disease study 2016," *Lancet Neurol*., vol. 18, no. 5, pp. 459–480, 2019.

[3] J. P. A. Joel, R. J. S. Raj, and N. Muthukumaran, "Review on Gait Rehabilitation Training using Human Adaptive Mechatronics System in Biomedical Engineering," in *Proc. Int. Conf. Comput. Commun. Informat. (ICCCI)*, Coimbatore, India, 2022, pp. 1-5.

[4] L. M. Mooney, E. J. Rouse, and H. M. Herr, "Autonomous exoskeleton reduces metabolic cost of human walking during load carriage," *Journal of Neuroengineering and Rehabilitation*, vol. 11, (1), pp. 80-80, 2014.

[5] Q. Wu, Z. Wang, and Y. Chen, "sEMG-Based Adaptive Cooperative Multi-Mode Control of a Soft Elbow Exoskeleton Using Neural Network Compensation," *IEEE Trans. Neural Syst. Rehabil. Eng.*, vol. 31, pp. 3384-3396, 2023.

[6] Q. Wu and Y. Chen, "Adaptive cooperative control of a soft elbow rehabilitation exoskeleton based on improved joint torque estimation," *Mech. Syst. Signal Process*., vol. 184, Feb. 2023, Art. no. 109748.

[7] K. Fitzsimons, A. M. Acosta, J. P. Dewald, and T. D. Murphey, "Ergodicity reveals assistance and learning from physical human-robot interaction," *Sci. Robot.*, vol. 4, no. 29, 2019.

[8] S. Rahman, S. Sarker, A. K. M. N. Haque, M. M. Uttsha, M. F. Islam, and S. Deb, "AI-Driven Stroke Rehabilitation Systems and Assessment: A Systematic Review," *IEEE Trans. Neural Syst. Rehabil. Eng*, vol. 31, pp. 192-207, 2023.

[9] Y. Zhu, Q. Wu, B. Chen, and Z. Zhao, "Design and voluntary control of variable stiffness exoskeleton based on sEMG driven model," *IEEE Robot. Autom. Lett.*, vol. 7, no. 2, pp. 5787–5794, Apr. 2022

[10] Q. Wu and Y. Chen, "Development of an intention-based adaptive neural cooperative control strategy for upper-limb robotic rehabilitation," *IEEE Robot. Autom. Lett.,* vol. 6, no. 2, pp. 335–342, Apr. 2021.

[11] Q. C. Wu, X. S. Wang, F. P. Du, and R. R. Xi, "Modeling and position control of a therapeutic exoskeleton targeting upper extremity rehabilitation," *Proc. Inst. Mech. Eng. C J. Mech. Eng. Sci.,* vol. 231, no. 23, pp. 4360–4373, 2017.

[12] S. Dalla Gasperina et al., "AGREE: A Compliant-Controlled Upper-Limb Exoskeleton for Physical Rehabilitation of Neurological Patients," *IEEE Trans. Med. Robot. Bionics*, vol. 5, no. 1, pp. 143-154, Feb. 2023.

[13] C. Fallaha, M. Saad, J. Ghommam, and Y. Kali, "Sliding Mode Control With Model-Based Switching Functions Applied on a 7-DOF Exoskeleton Arm," *IEEE/ASME Trans. Mechatronics*, vol. 26, no. 1, pp. 539-550, Feb. 2021.

[14] J. Kim, J. Kim, Y. Jung, D. Lee, and J. Bae, "A Passive Upper Limb Exoskeleton With Tilted and Offset Shoulder Joints for Assisting Overhead Tasks," *IEEE/ASME Trans. Mechatronics*, vol. 27, no. 6, pp. 4963-4973, Dec. 2022.

[15] Y. Zimmermann, M. Sommerhalder, P. Wolf, R. Riener, and M. Hutter, "ANYexo 2.0: A Fully Actuated Upper-Limb Exoskeleton for Manipulation and Joint-Oriented Training in All Stages of Rehabilitation," *IEEE Trans. Robot*., vol. 39, no. 3, pp. 2131-2150, June 2023.

[16] S. Li, Z. Wang, Z. Pang, Z. Duan, and M. Gao, "Design and analysis of an upper limb exoskeleton robot for stroke rehabilitation," in *Proc. IEEE Int. Conf. Real-time Comput. Robot. (RCAR)*, Guiyang, China, 2022, pp. 573-578.

[17] H. H. Cheng, T. M. Kwok, and H. Yu, "Design and Control of the Portable Upper-limb Elbow-forearm Exoskeleton for ADL Assistance," in *Proc. IEEE/ASME Int. Conf. Adv. Intell. Mechatronics (AIM)*, Seattle, WA, USA, 2023, pp. 343-349.

[18] Z. Zhang, T. Zhang, Y. Kan, and M. Xu, "Research on lower limb rehabilitation training device based on gravity balance," in *Proc. IEEE Int. Conf. Cyber Technol. Autom. Control Intell. Syst. (CYBER)*, Baishan, China, 2022, pp. 817-820.

[19] A. B. Halima, J. Bert, J. -F. Clément, and D. Visvikis, "Development of a 6 Degrees of Freedom Prostate Brachytherapy Robot with Integrated Gravity Compensation System," in *Proc. Int. Symp. Med. Robot. (ISMR)*, Atlanta, GA, USA, 2021, pp. 1-7.

[20] D. A. Streit, H. Chung, and B. J. Gilmore, "Perfect Equilibrators for Rigid Body Spatial Rotations About a Hooke's Joint," *ASME. J. Mech. Des*., vol. 113, no. 4, pp. 500-507, Dec. 1991.

[21] B. Siciliano, "Kinematic control of redundant robot manipulators: A tutorial," *J. Intell. Robot. Syst*., vol. 3, no. 3, pp. 201–212, 1990.

[22] Y. Guan and K. Yokoi, "Reachable Space Generation of A Humanoid Robot Using The Monte Carlo Method," *IEEE/RSJ Int. Conf. Robots Syst*., Beijing, China, pp. 1984–1989, 2006.

[23] S. J. Ball, I. E. Brown, and S. H. Scott, "MEDARM: a rehabilitation robot with 5DOF at the shoulder complex," in *Proc. IEEE/ASME Int. Conf. Adv. Intell. Mechatronics*, Zurich, Switzerland, 2007, pp. 1-6.

[24] G. Vazzoler, P. Bilancia, G. Berselli, M. Fontana, and A. Frisoli, "Analysis and Preliminary Design of a Passive Upper Limb Exoskeleton," *IEEE Trans. Med. Robot. Bionics*, vol. 4, no. 3, pp. 558-569, Aug. 2022.